Table 1. Clinical results of stereotactic radiotherapy for primary lung cancer

Author (year)	Total dose (Gy)	Daily dose (Gy)	Reference point	Local control	Median follow-up
Uematsu (2001)	50–60	10	80% margin	94% (47/50)	36 months
Arimoto (1998)	60	7.5	Isocenter	92% (22/24)	24 months
Timmerman (2003)	60	20	80% margin	87% (30/37)	15 months
Onimaru (2003)	48–60	6–7.5	Isocenter	80% (20/25)	17 months
Wulf (2004)	45–56.2	15–15.4	80% margin	95% (19/20)	10 months
This study (2005)	48	12	Isocenter	97% (44/45)	30 months

The primary indication for stereotactic radiotherapy in lung cancer could be a Stage Ia (T1N0M0) patient. Very early stage lung cancer can now be detected by screening CT examination, and these cases are also good indications for SRT. However, the issue of these cases is histologic confirmation. In our clinical experience, 7 of 95 total SRT cases could not be finally confirmed histologically. Of course, these seven cases are not included in this study. They could not be histologically confirmed because of the failure or difficulty in CT-guided biopsy or transbronchoscopic lung biopsy. CT screening has revealed very early staged lung cancer with ground glass opacity and some patients with severe emphysema could be contraindicated for biopsy. Therefore, the indication for SRT for these cases without histologic confirmation should be discussed in the future. When the tumor becomes larger than 3 cm in diameter, which corresponds to Stage Ib (T2N0M0), SRT is possible. However, the intratumor dose becomes less homogeneous, and the rate of occult distant metastases may increase. Therefore, the extension of the indication of this technique for T2 tumors requires more consideration for dose escalation or adjuvant chemotherapy.

CONCLUSION

The feasibility and accuracy of 3D conformal radiotherapy using a stereotactic body frame was evaluated. 3D SRT using a stereotactic body frame is a safe and effective treatment method for solitary lung tumors. Thus further clinical studies are warranted in future.

REFERENCES

1. Negoro Y, Nagata Y, Aoki T, *et al.* The effectiveness of an immobilization device in conformal radiotherapy for lung tumor: Reduction of respiratory tumor movement and evaluation of daily set-up accuracy. *Int J Radiat Oncol Biol Phys* 2001;50:889–898.
2. Nagata Y, Negoro Y, Aoki T, *et al.* Clinical outcomes of 3-D conformal hypofractionated single high dose radiotherapy for one or two lung tumors using a stereotactic body frame. *Int J Radiat Oncol Biol Phys* 52;1041–1046, 2002.
3. Aoki T, Nagata Y, Negoro Y, *et al.* Evaluation of CT appearance of lung injury after three-dimensional conformal stereotactic radiotherapy for solitary lung tumors. *Radiology* 2004; 230:101–108.
4. Ishimori T, Saga T, Nagata Y, *et al.* 18F-FDG and 11C-Methionine evaluation of the treatment response of lung cancer after stereotactic radiotherapy. *Ann Nuclear Med* 2004;18: 669–674.
5. Takayama K, Nagata Y, Negoro Y, *et al.* Treatment planning of stereotactic radiotherapy for solitary lung tumor. *Int J Radiat Oncol Biol Phys* 2005;61:1565–1571.
6. Blomgren H, Lax I, Goeranson H, *et al.* Radiosurgery for tumors in the body: Clinical experience using a new method. *J Radiosurg* 1998;1:63–74.
7. Lax I, Blomgren H, Larson D, *et al.* Extracranial stereotactic radiosurgery of localized target. *J Radiosurg* 1998;1:135–148.
8. Yaes RJ, Patel P, Maruyama Y. On using the linear-quadratic model in daily clinical practice. *Int J Radiat Oncol Biol Phys* 1991;20:1353–1362.
9. Therasse P, Arbuck SG, Eisenhauer EA, *et al.* New guidelines to evaluate the response to treatment in solid tumors. *J Natl Cancer Inst* 2000;92:205–216.
10. Uematsu M, Shioda A, Tahara K, *et al.* Computed tomography-guided frameless stereotactic radiotherapy for stage I non-small-cell lung cancer: A 5-year experience. *Int J Radiat Oncol Biol Phys* 2001;51:666–670.
11. Arimoto T, Usubuchi H, Matsuzawa T, *et al.* Small volume multiple non-coplanar arc radiotherapy for tumors of the lung, head, and neck and the abdominopelvic region. In: Lemke HU, editor. CAR '98 Computer assisted radiology and surgery. Tokyo: Elsevier; 1998. p. 257–261.
12. Timmerman R, Papiez L, McGarry R, *et al.* Extracranial stereotactic radioablation: Results of a phase I study in medically inoperable stage I non-small cell lung cancer. *Chest* 2003;124:1946–1955.
13. Onimaru R, Shirato H, Shimizu S, *et al.* Tolerance of organs at risk in small-volume, hypofractionated, image-guided radiotherapy for primary and metastatic lung cancers. *Int J Radiat Oncol Biol Phys* 2003;56:126–135.
14. Wulf J, Haedinger U, Oppitz U, *et al.* Stereotactic radiotherapy for primary lung cancer and pulmonary metastases: A noninvasive treatment approach in medically inoperable patients. *Int J Radiat Oncol Biol Phys* 2004;60:186–196.
15. Lung Cancer Study Group. Randomized trial of lobectomy versus limited resection for T1N0 non-small cell lung cancer. *Ann Thorac Surg* 1995;60:615–623.
16. Luketich JD, Ginsberg RJ. Limited resection versus lobectomy for stage I non-small cell lung cancer. In: Pass HI, Mitchell JB, Johnson DH, *et al.*, editors. Lung cancer: Principles and practice. Philadelphia: Lippincott-Raven; 1996. p. 561–566.
17. Onishi H, Araki T, Shirato H, *et al.* Stereotactic hypofractionated high-dose irradiation for stage I non-small cell lung carcinoma. *Cancer* 2004;101:1623–1631.
18. Graham MV. Predicting radiation response. *Int J Radiat Oncol Biol Phys* 1997;39:561–562.
19. Herfarth KK, Debus J, Lohr F, *et al.* Stereotactic single dose radiation treatment of tumors in the lung. *Radiology* 2000;217: 148.

ELSEVIER

Int. J. Radiation Oncology Biol. Phys., Vol. 61, No. 5, pp. 1565–1571, 2005

0360-3016/05/$–see front matter

doi:10.1016/j.ijrobp.2004.12.066

PHYSICS CONTRIBUTION

TREATMENT PLANNING OF STEREOTACTIC RADIOTHERAPY FOR SOLITARY LUNG TUMOR

KENJI TAKAYAMA, M.D., YASUSHI NAGATA, M.D., PH.D., YOSHIHARU NEGORO, M.D., TAKASHI MIZOWAKI, M.D., PH.D., TAKASHI SAKAMOTO, M.D., MASATO SAKAMOTO, M.D., TETSUYA AOKI, M.D., SHINSUKE YANO, PH.D., SACHIKO KOGA, R.T.T., AND MASAHIRO HIRAOKA, M.D., PH.D.

Department of Therapeutic Radiology and Oncology, Graduate School of Medicine, Kyoto University, Kyoto, Japan

Purpose: To analyze the stereotactic radiotherapy (SRT) plans in terms of internal target volume (ITV) and organs at risk (OARs).

Methods and Materials: Treatment planning and dose distributions were analyzed using dose–volume histograms (DVHs) of ITV and OARs in 37 patients, who were treated for a solitary lung tumor with SRT. The stereotactic body frame (SBF) was used for immobilization and accurate setup. Prescription dose was 48 Gy in four fractions at the isocenter.

Results: Use of SBF limits the extent of the noncoplanar beam directions to prevent a collision with the Linac gantry. DVH analyses showed that the homogeneity index, defined as the ratio of maximum and minimum dose to ITV, ranged from 1.03 to 1.25 (mean, 1.12). The volume irradiated with 20 Gy or more (V_{20}) of the lung ranged from 0.3 to 11.6% (mean, 4.4%) of the whole lung volume. The maximum dose to the other OARs ranged from 0 to 11.8 Gy (mean, 0.5–2.7) per fraction. No clinically significant complications were encountered.

Conclusions: Despite the limitation of the beam arrangement, a homogeneous target dose distribution, while avoiding high doses to normal tissues, was obtained. © 2005 Elsevier Inc.

Stereotactic radiotherapy, Lung tumor, Treatment planning, Dose–volume histogram, Normal tissue.

INTRODUCTION

Stereotactic radiotherapy (SRT) has recently been applied to patients with small lung tumors. Initial clinical results including ours were favorable, and local control rates around 90% have been reported (1–9).

Few reports, however, have been made about details of treatment planning—such as beam arrangement, dose distribution to the target, and tolerance dose of normal tissues. Regarding normal tissue, the use of a single high dose rather than a conventional dose in consideration of the biologic effect may increase the risk of complication. However, few cases with severe toxicity have been reported.

At Kyoto University, we have treated more than 80 patients with this method since July 1998, with the approval of our institutional review board and written informed consent provided by all patients. Our initial reports on daily setup accuracy and clinical results have already been published (5, 10). This article reports on our treatment planning procedures and results, especially in terms of doses to internal target volume (ITV) and organs at risk (OARs) using dose–volume histograms (DVHs) for the first half of cases.

METHODS AND MATERIALS

Treatment planning procedure

A stereotactic body frame (SBF) (Elekta AB, Stockholm, Sweden) was used as an immobilization device. We have previously reported the details of its use and its effect on daily setup accuracy and reduction of respiratory tumor motion (10).

The following describes the flow chart of our treatment planning procedures. First, the body of the patient was fixed by means of a vacuum pillow in SBF. The patient was set in the supine position with both arms raised using a T-shaped holding bar. The patient and SBF were set on the couch of an X-ray simulator to measure

Reprint requests to: Yasushi Nagata, M.D., Ph.D., Department of Therapeutic Radiology and Oncology, Graduate School of Medicine, Kyoto University, 54 Kawahara-cho, Shogoin, Sakyo-ku, Kyoto, 606-8507, Japan. Tel: (+81) 75-751-3418; Fax: (+81) 75-751-3418; E-mail: nag@kuhp.kyoto-u.ac.jp

Presented in part at the 6th International Stereotactic Radiosurgery Society Congress in Kyoto, Japan, June 22–26, 2003.

Supported by a grant-in-aid No.09255255, No.10153231, and No.13410183 of the Ministry of Education, Culture, Sports, Science and Technology, and No.23765293 of the Ministry of Health, Labor and Welfare in Japan.

Acknowledgments—The authors gratefully acknowledge Mr. Daniel Mrosek for his secretarial editorial assistance.

Received Mar 4, 2004, and in revised form Dec 7, 2004. Accepted for publication Dec 17, 2004.

tumor movement during free breathing using fluoroscopy. When the tumor moved more than 10 mm in the craniocaudal (C-C) direction, a small abdominal pressing plate called a "diaphragm control" was applied before computed tomography (CT) scanning, which suppresses the movement of the diaphragm and reduces tumor movement during respiration. CT images were then sequentially scanned from the neck to the upper abdomen with a CT simulator. The CT slice thickness and pitch were 1 to 3 mm each in the area of the tumor and 10 mm each in the other areas. Each CT slice was scanned with an acquisition time of 4 s to include the whole phase of one respiratory cycle. A series of CT images, therefore, included the tumor and its respiratory motion. The isocenter coordinate was defined using a three-dimensional radiation treatment planning system (3D RTPS) (CADPLAN R.6.0.8, Varian Associates, Palo Alto, CA). Anteroposterior (A-P) and lateral films for verification were then obtained using the X-ray simulator at a designated isocenter. Because the CT simulator and the X-ray simulator employed the same couch in our integrated system, the patient's position on verification films was the same as that on CT images in relation to SBF (10).

The outlines of the target were delineated on 3D RTPS using lung CT window settings (window width 2000 Hounsfield units (HU) and window level −700 HU, typically). A physician delineated both the solid area (tumor itself), which could be seen even using mediastinal CT window settings (window width 350 HU and window level 40 HU, typically), and the surrounding obscure area, which could be seen only under lung CT settings. The obscure area is important because it indicates either tumor microscopic invasion or respiratory tumor motion. This target volume corresponded to the ITV in International Commission on Radiation Units and Measurements Report 62. The outlines of gross tumor volume and clinical target volume were included in the ITV, and gross tumor volume and clinical target volume could not be delineated on the planning CT in our system because the CT images already included the internal motion. Spiculation and pleural indentation were included within the ITV. Neither mediastinal nor hilar lymph nodes were included within the ITV.

The physician also delineated the outline of the following OARs: lung, spinal cord (canal), pulmonary artery, heart, and esophagus. The outline of the lung included that of the target. The pulmonary artery, heart, and esophagus were delineated with each outer contour and included both the wall and content of each organ. The pulmonary artery was delineated from its origin to the pulmonary hila. The esophagus was delineated from the level of the sternal notch to the esophagocardial junction.

Treatment planning was performed using the 3D RTPS, and 5–10 noncoplanar static ports were selected. Edges of the multileaf collimator (MLC) were located 8–10 mm outside of the ITV in the C-C direction and 5 mm in the A-P and lateral directions. The distance in the C-C direction was larger than that in the other directions, because the former was set to compensate for an irregular respiratory motion which could not be included in the ITV using the CT scan with the acquisition time of 4 s. The prescribed dose was 12 Gy per fraction at the isocenter, and the total dose was 48 Gy with four fractions. The dose was delivered by a linear accelerator (CLINAC 2300 C/D, Varian medical systems) with 6-MV photons. Each MLC had a 1-cm leaf width at the isocenter. One of the planning goals was to maintain a dose homogeneity of ITV within 10%, which meant a dose to ITV ranging from 90% to 110% of the isocenter dose. Another goal was to maintain V_{20} (the volume irradiated with 20 Gy or more) of the bilateral lung at less than 25%. Beam arrangement was also selected to minimize doses to OARs. The use of the beam that passed directly through the spinal cord was avoided.

Beam arrangement

The applicable area of noncoplanar beam directions is more limited in SRT for extracranial tumors compared with intracranial tumors. There are three main causes: *(1)* risk of collision of the couch and the gantry; *(2)* blockade of the contralateral posterior beams by the supporting metal bar at the couch center; and *(3)* usage of the SBF that might cause the additional collision with the gantry. Figure 1 shows examples of the applicable gantry angle range that varies depending on the couch angle. We usually shift the position of the supporting couch and SBF in the lateral direction to avoid the metal bar on the center of the couch for a posterior beam, as shown in Fig. 2a. The figure shows the scheme of the couch and SBF shift from the foot-side view, in which the couch is shifted to the left side by 16.5 cm, and the SBF is shifted to the right side by 6.5 cm to put the center of the right-sided target on the isocenter. To find the applicable beam directions on the 3D RTPS more easily, we made diagrams that indicated applicable combinations of couch and gantry angles (11). Fig. 2b shows the diagram for the right-sided tumor. The area between an upper line and a lower line presents the applicable combination of the gantry and couch angles in each different isocenter height from the SBF base that determines the couch height. The diagrams were very useful in finding applicable beam directions at the time of treatment planning.

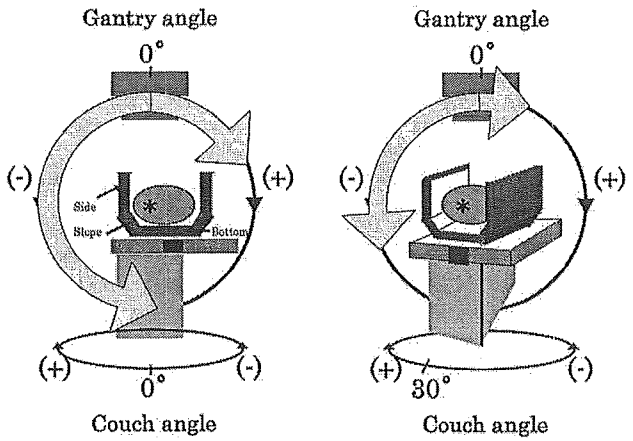

Fig. 1. Limitation of the couch and gantry angles. The left figure shows the applicable gantry position when the couch is set to the standard position (0° of the couch angle) and the tumor is in the right lung. The beam from the left direction cannot be used either because of the collision of the gantry and the couch or SBF. The beam from the posterior direction cannot be used either because of the interference of the supporting bar that lies in the center of the couch. Therefore, the applicable gantry angles are limited in the range of the thick arrow. Larger we set the couch rotation angle (e.g., 30° as shown in the right figure of Fig. 1), wider gets the zone in which the gantry and either the couch or stereotactic body frame mutually interfere. The range of the applicable gantry angle, therefore, is limited further as the thick arrow shows in the right figure. The supporting bar at the couch center is shown as a black square. The outer stiff frame of the stereotactic body frame consists of bilateral "side" walls, a "bottom" wall, and "slope" walls between the side and the bottom.

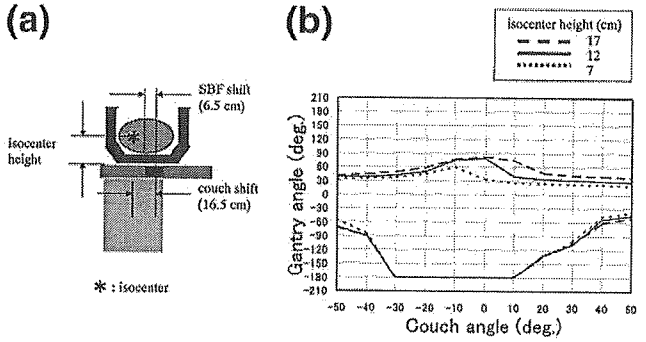

Fig. 2. Diagrams of beam arrangements. (a) Scheme of the couch and stereotactic body frame shift, which is necessary to avoid the metal bar on the center of the couch for a posterior beam. Isocenter height from the stereotactic body frame base is the parameter determining the couch height. (b) The applicable area of beam arrangement at the different isocenter heights. The area between each sequential line presents the applicable combination of the gantry and couch angles.

The procedure for choosing the optimal beam arrangement was forward planning based on our experiences. The beam arrangement used in our planning consisted of 5–10 beams, which included 1–4 coplanar beams and 2–6 noncoplanar beams. The alignment of the beams was chosen to be geometrically homogeneous wherever possible within the limitation. The use of opposing beams was avoided. The use of the beam that passed directly through the spinal cord was also avoided, although just one of the beams is allowed to pass directly through the spinal cord in recent planning. After checking the dose distribution by means of both DVH and dose distribution on axial images, modification of the beam alignment, number of beams, and weight of each beam was made to create an optimal dose distribution, which showed homogenous distribution to the target and low dose distribution to the normal tissues. A typical beam arrangement and the dose distribution are shown in Fig. 3 and Table 1.

Dose correction

There are two important issues for dose correction in SRT for lung tumors. One is lung inhomogeneity correction; the other is correction for dose attenuation caused by SBF.

We use the generalized Batho method to calculate the dose distribution with lung inhomogeneity correction. The center dose of lung tumors calculated by 3D RTPS without lung inhomogeneity correction were higher than the dose calculated with a house-made Monte Carlo simulation by 6% as an average (range 1–14%) in our institutional experiment. In contrast, the dose calculated with the generalized Batho method almost corresponded to the dose calculated with the Monte Carlo simulation. When the radiation field became too small, the dose calculated with the generalized Batho method did not correspond to the actual dose. Therefore, we did not use a radiation field smaller than 3 cm × 3 cm.

Another experiment revealed that the beams passing through the SBF showed a considerable dose reduction, although the frame, which has a honeycomb structure with a center of paper and surrounding glass fiber surface with edgings of pure birch, absorbs fewer X-rays compared with other materials. The outer stiff frame of the SBF consists of bilateral side walls, a bottom wall, and sloped walls between the side and bottom, as shown

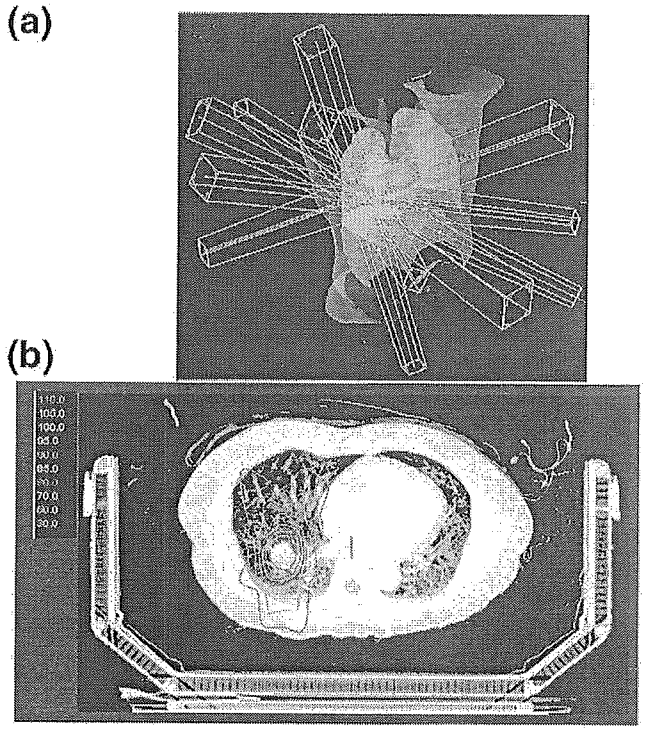

Fig. 3. A typical beam arrangement and the dose distribution. (a) A three-dimensional figure of a typical beam arrangement consisting of two coplanar beams and four noncoplanar beams. The detail of the gantry and the couch angles are shown in Table 1. (b) The two-dimensional dose distribution using this beam arrangement.

in Fig. 1. In the experiment, the mean dose attenuation ratio through each part of the frame was 7.5% for the side wall, 10.6% for the sloped wall, 9.5% for the bottom wall, 11.9% for transitional part between the side and sloped wall, and 11.8% for the transitional part between the sloped and bottom wall. The dose attenuation ratio ranged from 6.0 to 15.4%, and the mean value was 9.3%. Therefore, we used a uniform dose correction of 9.3% for beams passing through SBF in clinical use. According to another experiment using a phantom, the uniform dose correction of 9.3% minimized the dose difference from the actual dose by less than 3% (11).

Analysis of treatment planning

We analyzed the plans of 37 consecutive patients who underwent hypofractionated single high-dose SRT for small lung tumors at our institute between October 1998 and December 2000. All tumors were located at periphery of the lung and were of sizes smaller than 4 cm in the largest diameter on a diag-

Table 1. A typical beam arrangement

Port no.	Gantry angle	Couch angle (degrees)
1	180	0
2	260	0
3	340	40
4	30	40
5	35	320
6	295	320

nostic CT image or radiograph. In the analysis of target dose, we evaluated maximum dose, minimum dose, 90% coverage volumes, and homogeneity index. Homogeneity index was defined as the ratio of maximum dose to minimum dose. In the analysis of dose to the lung, we evaluated the V_{20} as an index related to the risk of radiation pneumonitis. In the analysis of dose to the other normal tissues, we evaluated maximum dose and mean dose to the spinal cord, heart, esophagus, and pulmonary artery. The median (range) clinical follow-up was 32 (3–63) months.

RESULTS

Target dose

The ITV ranged from 0.3 to 41.3 mL (mean, 13.4 mL). The ITV maximum dose ranged from 100.0 to 107.5% (mean, 102.6%), and the ITV minimum dose ranged from 82.5 to 99.2% (mean, 92.0%). The homogeneity index ranged from 1.03 to 1.25 (mean, 1.12). Figure 4 shows the relationship of the target volume with minimum dose, maximum dose, and homogeneity index for all patients. The minimum dose generally decreased as the target volume increased (coefficient of determination: $r^2 = 0.53$). On the other hand, the homogeneity index increased as well, because the index nearly equaled to the inverse number of the minimum dose ($r^2 = 0.59$). When the ITV exceeded 30 mL, the minimum dose was less than 90% and the homogeneity index was more than 1.2 in all cases. The percentage of the target volume irradiated with a dose of 90% or more of the isocenter dose (90% coverage volumes) exceeded 99.5% in all patients but one, whose ITV exceeded 40 mL.

Dose to the normal tissues

Doses to the normal tissues were analyzed for the lung, spinal cord, esophagus, heart, pulmonary artery, and bronchus. The results are summarized in Table 2, except for the dose to the lung.

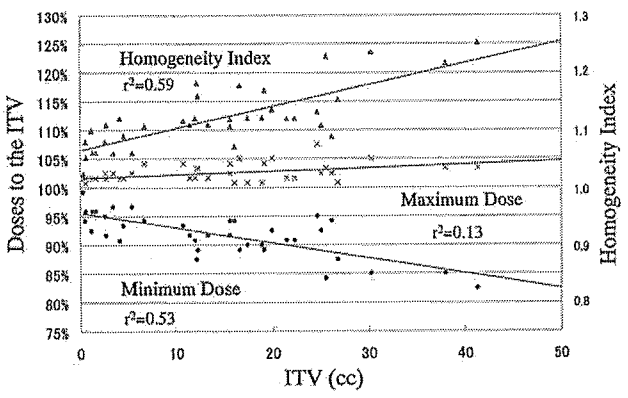

Fig. 4. Correlation with the internal target volume (ITV) and the dose to the ITV. Minimum and maximum doses to the ITV and homogeneity indices in each patient are presented in association with the value of ITV. Minimum dose had the tendency to decrease as the target volume increased ($r^2 = 0.53$). Homogeneity index had also a tendency to increase ($r^2 = 0.59$).

Table 2. Dose to the normal tissues

	Mean dose	Max dose
	Mean (range) Gy/fraction	
Esophagus	0.5 (0.0–1.3)	1.9 (0.1–5.2)
Bronchus	0.8 (0.0–5.0)	1.8 (0.1–7.9)
Pulmonary artery	0.8 (0.1–1.5)	2.6 (0.1–11.8)
Heart	0.3 (0.0–1.5)	2.7 (0.1–10.6)
Spinal cord	0.1 (0.0–0.2)	0.5 (0.0–2.2)

Mean and maximum doses of the normal tissues in each plan are summarized in this table. The values outside and between parentheses represent the average and the range for all patients, respectively.

Lung. V_{20} of the whole lung ranged from 0.3% to 11.6% with a mean value of 4.3%. There were 3 patients whose V_{20} exceeded 10%. One of them had only one lung because of tuberculosis. The other 2 patients had larger tumors than all other patients. Figure 5 shows the relationship of the target volume with V_{20} of the whole lung in all patients. In most of the patients, V_{20} increased in proportion to the target volume. Some patients, however, showed much larger V_{20} than patients with the same target volume when the tumor was located near the center of the lung. On the other hand, some patients showed smaller V_{20} when the tumor was located near the chest wall. Regarding pulmonary toxicity, only 2 patients (5%) had Grade 2 radiation pneumonitis in the National Cancer Institute - Common Toxicity Criteria (NCI-CTC), and no patients had more than Grade 2 pneumonitis. Thirty-four patients (92%) showed Grade 1 radiation pneumonitis, and most of them were asymptomatic and had only pneumonitis changes on CT images.

Spinal cord. A low dose to the spinal cord was maintained, because the use of beams that pass through the cord directly was intentionally avoided. The maximum dose in all patients was only 2.2 Gy per fraction. No patients showed cord toxicity.

Esophagus. The maximum dose to the esophagus in all patients was 5.2 Gy per fraction. The dose to the esophagus exceeded 5 Gy per fraction (20 Gy in total dose) only for the patient who showed the maximum dose. No severe esophageal toxicity greater than NCI-CTC Grade 2 was encountered.

Heart. The maximum dose to the heart in all patients was 10.6 Gy per fraction. The maximum volume of the heart irradiated over 5 Gy per fraction was 7.2 mL in the same patient. There were 5 patients whose maximum dose to the heart exceeded 5 Gy per fraction. In 3 of the 5 patients, more than 1 mL was irradiated with 5 Gy per fraction, and DVHs are shown in Fig. 6a. No severe cardiovascular toxicity greater than NCI-CTC Grade 2 was encountered.

Pulmonary artery. The maximum dose to the pulmonary artery in all patients was 11.2 Gy per fraction. The patient who showed the maximum dose to the pulmonary artery had a tumor near the pulmonary hilum. The volume irradiated

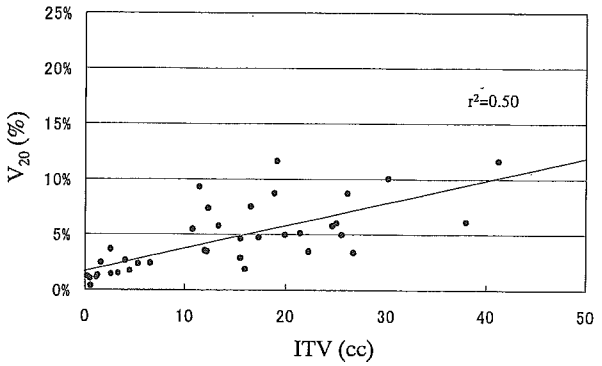

Fig. 5. Correlation with the internal target volume (ITV) and the volume irradiated with 20 Gy or more (V_{20}) of the lung. V_{20} had a tendency to increase as ITV increased (r^2 = 0.50). However, V_{20} also depended on the total lung volume and tumor position.

with 5 Gy or more was 5.13 mL, and the volume irradiated with 10 Gy or more was 0.86 mL in this patient. Dose to the pulmonary artery exceeded 5 Gy in 14 patients, the volume irradiated with 5 Gy or more exceeded 1 mL in 7 patients, whose DVH are shown in Fig. 6c. No clinical toxicity such as pulmonary bleeding or pulmonary artery obstruction was encountered.

Bronchus. Maximum dose to the bronchus in all patients was 7.9 Gy, and the maximum volume irradiated with 5 Gy or more was 2.92 mL. Figure 6b shows the DVH of the patient who was irradiated with the maximum dose to the bronchus. Though dose to the bronchus exceeded 5 Gy in 5 patients, the volume irradiated with 5 Gy or more did not exceed 1 mL except in the patient previously mentioned. No clinical toxicity such as symptomatic bronchitis or bronchial stenosis was encountered.

DISCUSSION

Stereotactic body frame was originally developed by Blomgren and Lax at Karolinska Hospital in Sweden (12, 13). It gives the following advantages: *(1)* Effective patient immobilization during treatment; *(2)* greater daily setup accuracy; *(3)* easy setup correction because of measuring scales on the frame; and *(4)* successful reduction of the respiratory tumor movement with a small abdominal pressing plate. Daily setup accuracy is much more important for SRT than for conventional radiotherapy, because a setup error in single treatment causes a larger error in total dose distribution. Its accuracy has been proven to be high enough in many articles, although verification and repositioning at every treatment are recommended (10, 12, 14). Its effectiveness on the reduction of respiratory tumor movement has also been proven in some articles (10, 14). On the other hand, this frame has the following disadvantages: excessive time required to arrange stereotactic coordinates; inappropriate application for obese patients; or limited availability of beam arrangement. The last disadvantage was considered an issue that should be solved before starting the practice of SRT with SBF. Therefore, we made the diagrams for available combinations of couch and gantry angles to use in routine clinics (11). We configured 5–10 noncoplanar beams using the diagrams, aiming for a practicable and balanced arrangement under the limitation. The diagrams were helpful in avoiding the selection of unusable beams in actual treatment.

We routinely use noncoplanar multiple static ports. The number of ports depends on the tumor size and location and is selected from 5 to 10 in our plan. Although a large number of ports makes dose distribution more conformal compared with a small number in general, our simulation revealed that it has made little difference in the increase of the number of ports more than 10 under the limitation of the couch and gantry arrangement. Moreover, because radiotherapy staff member enter the treatment room for checking that there is no collision when the gantry or the couch are moved, the large number of ports increases both treatment time and workload of the staff. These are the reasons why we use 5–10 static ports. Despite the limitation of the beam arrangement because of usage of the body frame and the supporting metal bar in the center of the couch, appropriate dose distributions were successfully achieved. Dose homogeneity indices for ITV were very small, and 90% dose coverage volumes were more than 99.5% in all cases except one.

The multiple arc technique is applied to SRT for extracranial tumors in a few institutes (15). However, there were some problems using this technique in our institute. Because the available beam range was limited by the SBF and couch structure, sufficient gantry rotational angles were not available. Also, the dose attenuation correction was practically impossible for an arc that contained both beams that passed and those that did not pass through the SBF. In our fundamental experiment for comparing the dose distribution between multiple static ports (6, 8, or 10 ports) and multiple arcs (3, 5, or 7 arcs, 300°), few differences were observed

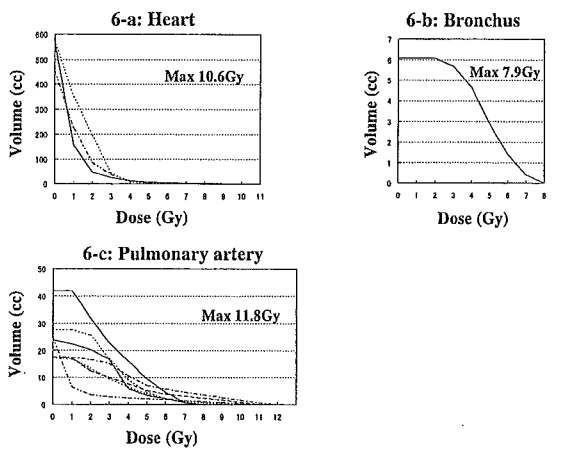

Fig. 6. Dose–volume histogram of the normal tissues. The dose–volume histogram of patients irradiated with more than 5 Gy to 1 mL or more of each normal tissue. (a) Heart. (b) Bronchus. (c) Pulmonary artery.

between both techniques in SRT for extracranial tumors under the constraints mentioned here. Therefore, we routinely use noncoplanar multiple static ports.

In regard to normal tissues, Emami *et al.* reported tolerance doses at a 5% complication rate in 5 years (TD 5/5) when irradiated with 2 Gy per fraction (16). This result, however, may not be applicable to hypofractionated, single, high-dose radiotherapy. Some recent articles reported on normal tissue complications in SRT for lung tumors. Severe toxicities are summarized in Table 3 (3, 4, 6, 13, 17). There are, however, few articles that have reported on the relationship between doses to normal tissues and their complications.

For lung doses, Graham *et al.* compared the total lung DVH parameters with the incidence and grade of pneumonitis after treatment for non–small-cell lung cancer. They concluded that V_{20} might be useful in comparing competing treatment plans to evaluate the risk of pneumonitis (18). We have used V_{20} of the total lung volume as a dose constraint for the lung. V_{20} was sufficiently lower than the dose constraint (25%) in our planning. We have encountered only 2 patients who showed radiation pneumonitis of Grade 2 in the NCI-CTC version 2.0, and no patients who showed Grade 3 or more. It is, however, controversial whether V_{20} can be applied to SRT in the same way as it is applied to conventional radiotherapy. We must follow this up carefully and analyze other parameters when severe toxicity occurs in the future.

A low dose to the esophagus was maintained in our planning, and no toxicity has yet been seen. Onimaru *et al.* have reported a patient who died because of a radiation-induced esophageal ulcer after receiving 48 Gy in eight fractions (6). The review of the planning revealed that 1 mL of the esophagus might have received 42.5 Gy with a maximum dose of 50.5 Gy. Though the case of this patient may have indicated the tolerance dose, they could not determine the essential maximum tolerance dose of the esophagus because of uncertainty in the contouring.

Wulf *et al.* reported fatal bleeding from the pulmonary artery 9 months after stereotactic irradiation (Grade 5) in a patient who received a previous conventional irradiation with a total dose of 60 Gy and stereotactic irradiation with a total dose of 30 Gy per 10 fractions. In our study, dose to the pulmonary artery was relatively higher when the tumor was located near the pulmonary hilum. Five Gy per fraction in more than 1 mL was irradiated in 5 of 7 patients. Severe toxicity has not yet been presented. The true volume of a pulmonary arterial wall irradiated with 5 Gy in the patients was smaller than the volume containing arterial blood used in our analysis. This might be one of the reasons why there has been no severe toxicity. However, the true tolerance dose to the pulmonary artery is still unknown.

Dose to the bronchus using brachytherapy has been reported to be from 4 to 6 Gy at a reference point per fraction with four fractionations in some typical protocols in other institutes. The reference point was typically located at a 5-mm depth from the mucosal surface, and more doses were irradiated at the mucosal surface. Our dose to the bronchus was considered to be much safer in comparison with these reports.

A low dose to the spinal cord was maintained in our planning because the use of the beam that included the spinal cord in the beam pathway was avoided. No patient with radiation myelitis has been reported after SRT. We changed the strategy of the beam arrangement and allowed just one of the beams to pass directly through the spinal cord in recent planning to improve the dose distribution for the target. One beam delivered a dose of about 2 Gy or less per fraction to the cord, when the fractional dose of 12 Gy was evenly delivered by six ports.

There is no report to be referred to regarding severe toxicity of the heart after stereotactic single high dose radiotherapy. In our study, although part of the heart was irradiated with a high dose in some patients, no severe complication has been encountered. However, the effect of high-dose irradiation to the coronary artery remains unclear, and the risk of severe toxicity may increase when a patient suffers from arterial atherosclerosis. Therefore, we must follow patients carefully over a long period. In regard to skin reaction, 7 patients (19%) showed erythema or pigmentation denoting Grade 1 acute toxicity at the entrance of a beam. No patient showed skin toxicity with Grade 2 or more.

Tolerance dose to OARs in SRT is a great concern for

Table 3. Severe toxicities (Grade 3 or more)

Authors	No. of targets (patients)	Dose/fraction at isocenter	Severe toxicities
Blomgren *et al.*	17 (13)	23–68 Gy/1–3 Fr.	Grade 3: Chronic cough (6%)
Hara *et al.*	23 (19)	20–30 Gy/1 Fr. (minimum to GTV)	Grade 3: Respiratory symptom (O_2 supply) (4%)
Onimaru *et al.*	57 (45)	48–60 Gy/8 Fr.	Grade 5: Esophageal ulcer (2%)
Wulf *et al.*	27	45 Gy/3 Fr.	Grade 3: Esophageal ulcer (4%) Grade 5: Pulmonary artery bleeding (4%)
Gomi *et al.*	38 (35)	40–62.5 Gy/4–5 Fr.	Grade 4: Pneumonitis (3%) Grade 4: Dermatitis (3%) Grade 3: Esophagitis (3%)

Abbreviations: Fr. = fraction; NCI-CTC = National Cancer Institute - Common Toxicity Criteria.

Severe toxicities of Grade 3 or more in NCI-CTC are summarized in this table. All of the authors in the table used three-dimensional conformal radiotherapy for lung tumors using hypofractionation or single fractionation shown in the table.

radiation oncologists. However, it could not be determined in our study, because we did not encounter any severe toxicity.

Verification is a very important process, especially in hypofractionated stereotactic radiotherapy. Negoro *et al.* previously reported the details of our verification method and the results of setup error (10). We used A-P and lateral verification films obtained by a X-ray simulator after CT scan, to compare linacography (A-P and lateral port films) immediately before irradiation. X-ray simulation films have a higher resolution than digital reconstructed radiography, especially in the C-C direction. X-ray simulation films can be easily taken using our integrated system, in which the CT simulator and the X-ray simulator are employed on the same couch. Therefore, we used X-ray simulation films to verify patient setup.

Dose correction for lung inhomogeneity is still a controversial issue. The application of the Monte Carlo calculation method to routine clinics in the future is one of the solutions. In the present situation, we consider that dose correction using a method such as the generalized Batho method should be performed to deliver the true prescribed dose.

Target delineation and definition are other important issues in SRT for lung tumors. Interobserver variation in target delineation is not negligible in some cases. There has been no universal target definition for small solitary lung tumor in SRT. Although the only concept is proposed by International Commission on Radiation Units and Measurements Report 62, details of target definition depend on the treatment methods, such as the way to scan the CT of the tumor and the verification method. Further discussions on these issues are necessary.

In conclusion, the use of multiple noncoplanar static ports achieved homogeneous target dose distribution and avoided high dose to normal tissues, despite the limitation of the beam arrangement from the use of the body frame and couch structure. Tolerance doses to the normal tissues are yet unknown when using single high-dose irradiation. Therefore, we should continue to make treatment plans carefully. In addition, further follow-ups of clinical cases are required to know the tolerance dose to the normal tissues in stereotactic radiotherapy.

REFERENCES

1. Uematsu M, Shioda A, Tahara K, *et al.* Focal, high dose, and fractionated modified stereotactic radiation therapy for lung carcinoma patients: a preliminary experience. *Cancer* 1998; 82:1062–1070.
2. Nakagawa K, Aoki Y, Tago M, *et al.* Megavoltage CT-assisted stereotactic radiosurgery for thoracic tumors: original research in the treatment of thoracic neoplasms. *Int J Radiat Oncol Biol Phys* 2000;48:449–457.
3. Wulf J, Hadinger U, Oppitz U, *et al.* Stereotactic radiotherapy of targets in the lung and liver. *Strahlenther Onkol* 2001;177: 645–655.
4. Hara R, Itami J, Kondo T, *et al.* Stereotactic single high dose irradiation of lung tumors under respiratory gating. *Radiother Oncol* 2002;63:159–163.
5. Nagata Y, Negoro Y, Aoki T, *et al.* Clinical outcomes of 3D conformal hypofractionated single high-dose radiotherapy for one or two lung tumors using a stereotactic body frame. *Int J Radiat Oncol Biol Phys* 2002;52:1041–1046.
6. Onimaru R, Shirato H, Shimizu S, *et al.* Tolerance of organs at risk in small-volume, hypofractionated, image-guided radiotherapy for primary and metastatic lung cancers. *Int J Radiat Oncol Biol Phys* 2003;56:126–135.
7. Hof H, Herfarth KK, Munter M, *et al.* Stereotactic single-dose radiotherapy of stage I non-small-cell lung cancer (NSCLC). *Int J Radiat Oncol Biol Phys* 2003;56:335–341.
8. Whyte RI, Crownover R, Murphy MJ, *et al.* Stereotactic radiosurgery for lung tumors: preliminary report of a phase I trial. *Ann Thorac Surg* 2003;75:1097–1101.
9. Takai Y, Mituya M, Nemoto K, *et al.* [Simple method of stereotactic radiotherapy without stereotactic body frame for extracranial tumors]. *Nippon Igaku Hoshasen Gakkai Zasshi* 2001;61:403–407.
10. Negoro Y, Nagata Y, Aoki T, *et al.* The effectiveness of an immobilization device in conformal radiotherapy for lung tumor: reduction of respiratory tumor movement and evaluation of the daily setup accuracy. *Int J Radiat Oncol Biol Phys* 2001;50: 889–898.
11. Koga Y, Yano S, Okada T, *et al.* Stereotactic radiotherapy using a stereotactic body frame: research on effective irradiation angle and correcting dose. *Nippon Hoshasen Gijutsu Gakkai Zasshi* 2001;57:1395–1405.
12. Lax I, Blomgren H, Naslund I, *et al.* Stereotactic radiotherapy of malignancies in the abdomen. Methodological aspects. *Acta Oncol* 1994;33:677–683.
13. Blomgren H, Lax I, Naslund I, *et al.* Stereotactic high dose fraction radiation therapy of extracranial tumors using an accelerator. Clinical experience of the first thirty-one patients. *Acta Oncol* 1995;34:861–870.
14. Herfarth KK, Debus J, Lohr F, *et al.* Extracranial stereotactic radiation therapy: set-up accuracy of patients treated for liver metastases. *Int J Radiat Oncol Biol Phys* 2000;46:329–335.
15. Uematsu M, Shioda A, Suda A, *et al.* Computed tomography-guided frameless stereotactic radiotherapy for stage I non-small cell lung cancer: a 5-year experience. *Int J Radiat Oncol Biol Phys* 2001;51:666–670.
16. Emami B, Lyman J, Brown A, *et al.* Tolerance of normal tissue to therapeutic irradiation. *Int J Radiat Oncol Biol Phys* 1991;21:109–122.
17. Gomi K, Koichi M, Oguchi M, *et al.* Clinical experience of stereotactic radiation therapy for stage Ia non-small cell lung cancer [abstract]. 6th International Stereotactic Radiosurgery Society Congress, Kyoto, Japan, June 22–26, 2003; 146.
18. Graham MV, Purdy JA, Emami B, *et al.* Clinical dose-volume histogram analysis for pneumonitis after 3D treatment for non-small cell lung cancer (NSCLC). *Int J Radiat Oncol Biol Phys* 1999;45:323–329.

Breast Cancer
Vol. 12 No. 2 April 2005

Original Article

Bilateral Breast-Conserving Therapy for Bilateral Breast Cancer: Results and Consideration of Radiation Technique

Chikako Yamauchi[*1], Michihide Mitsumori[*1], Yasushi Nagata[*1], Masaki Kokubo[*2], Takashi Inamoto[*3], Keiichi Mise[*4], Hiroshi Kodama[*4], and Masahiro Hiraoka[*1]

*[1]Department of Therapeutic Radiology and Oncology, Graduate School of Medicine, Kyoto University, *[2]Department of Image-based Medicine, Institute of Biomedical Research and Innovation. Kobe, Japan, *[3]Gastroenterological Surgery, Graduate School of Medicine, Kyoto University, *[4]Kodama Breast Clinic, Kyoto, Japan.

Background: Although breast-conserving surgery followed by definitive irradiation is an established treatment for patients with early breast cancer, the role of breast-conserving therapy (BCT) for patients with bilateral breast cancer has not been well studied and the radiation therapy technique is still under investigation. We examined the feasibility of breast-conserving therapy for bilateral breast cancer and present here our radiation therapy technique with CT simulator.

Methods: Between July 1990 and December 1998, we treated 17 patients with bilateral breast cancer who underwent bilateral breast-conserving surgery followed by definitive irradiation. Seven patients had synchronous bilateral breast cancer and ten had metachronous bilateral breast cancer. Radiation therapy consisted of 50 Gy to the bilateral whole breast in all patients but one. A CT simulator was used to plan a tangential radiation field to the breast in all patients. Boost irradiation of 10 Gy was administered to 8 tumors with close or positive margins.

Results: With a median follow-up periods of 95 months from each operation, no patients showed loco-regional recurrence on either side, and none suffered distant metastasis. Furthermore no serious late adverse effects were observed.

Conclusion: This study demonstrated that BCT is feasible for bilateral breast cancer and the CT simulator is useful for determining the radiation field, especialy when lesions are metachronous.

Breast Cancer 12:135-139, 2005.

Key words: Bilateral breast cancer, Breast-conserving therapy, BCT, Breast-conserving surgery, Radiation therapy

The incidence of clinically observed bilateral breast cancer is reported to range from 1.4 to 11.8%[1-3], small but significant. Although breast-conserving surgery followed by irradiation is an established treatment for patients with early breast cancer, the frequency of patients receiving bilateral breast irradiation ranges from 0.4% to 5.5%[4-6]. The role of breast-conserving therapy for patients with bilateral breast cancer has not been well studied and scant attention has been devoted to the techniques for radiation therapy. We herein present our technique, which utilizes a CT simulator, and analyze the outcome of treatment for patients with bilateral breast cancer treated with breast-conserving therapy (BCT).

Reprint requests to Chikako Yamauchi, Department of Therapeutic Radiology and Oncology Graduate School of Medicine, Kyoto University 54 Kawahara-cho, Shogoin, Sakyo, Kyoto, 606-8507, Japan.
E-mail: chikay@kuhp.kyoto-u.ac.jp

Abbreviations:
BCT, Breast -conserving therapy

Received June 1, 2004; accepted November 24, 2004

Materials and Methods

Between July 1990 and December 1998, a total of 1036 patients with breast cancer were treated with BCT, defined as breast-conserving surgery and axillary lymph node dissection followed by definitive radiation therapy at the Department of Radiology at Kyoto University Hospital. Among them, 35 patients (3.4%) had bilateral breast cancer, and 17 of them were treated with bilateral BCT (Fig 1). Therefore, 17 patients treated with bilateral BCT were analyzed in the present study.

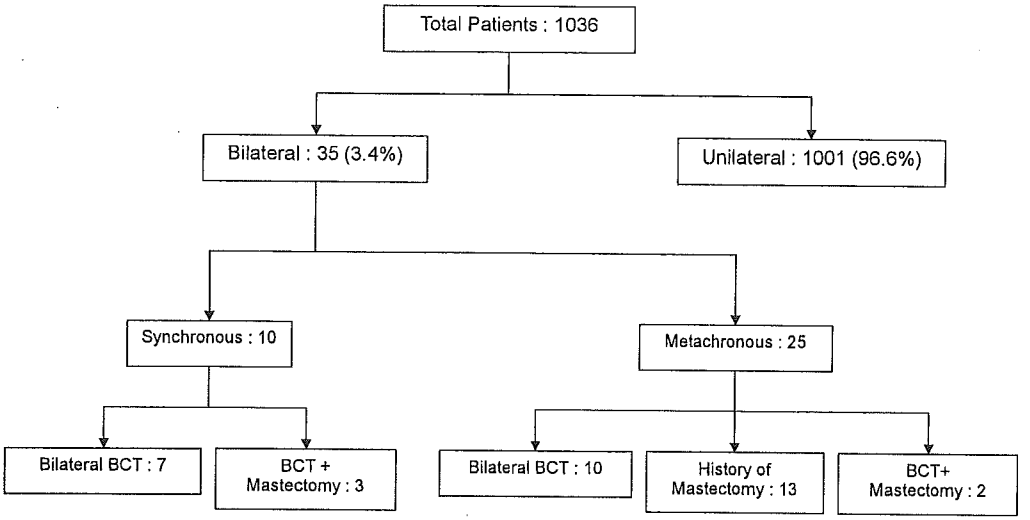

Fig 1. Total patients treated between July 1990 and December 1998.

Table 1. Patient Characteristics

	Synchronous (7 Pt.)	Metachronous (10 Pt.)
Age at diagnosis	Median 53 (43-68)	Median 45 (28-54)*
Family history		
1st degree	0	3
2nd degree	1	0
Menstrual status		
Premenopausal	2	8
Perimenopausal	0	0
Postmenopausal	2	2
Unknown	1	

* age at the diagnosis of the 1st tumor

Table 2. Tumor Characteristics of the 34 Treated Breasts

	Number	%
Pathology		
DCIS	1	
Invasive ductal	32	94
Invasive lobular	1	
Clinical T Stage		
T0	1	3
T1	22	65
T2	11	32
Clinical UICC Stage		
I	22	65
IIA	9	26
IIB	3	9
Pathologic N stage		
N0	31	91
N1	3	9
Estrogen receptor status		
Negative	11	32
Positive	13	38
Not done/unknown	10	30

Seven patients had synchronous bilateral breast cancer and 10 patients had metachronous bilateral breast cancer. They developed the newly diagnosed contralateral breast cancer 4 to 70 months after the first BCT with a median interval of 29 months. Synchronous breast cancer was defined as the diagnosis of both tumors within 1 month. The patients' characteristics and the characteristics of the 34 breast cancers are summarized in Tables 1 and 2.

As regards conservative surgery, 14 tumors were treated by quadrantectomy, while 20 tumors were treated by wide excision. All patients underwent axillary dissection bilaterally. Twenty-six tumors had negative margins of resection, 6 had close margins of resection, that is, within 5 mm from the resected margin, and 1 had positive margins of resection, defined as microscopic involvement at the resected margin on the histological examination.

Following breast conserving surgery, a total dose of 50 Gy in daily fractions of 2 Gy was delivered over 5 weeks to the whole breast via opposing tangential fields. We used a CT simulator (Shimadzu Corp. CT-S, Kyoto) to plan the tangential

fields. We selected the beam energy for the tangential fields according to the breast size: twenty-seven unilateral breasts were treated with cobalt-60 gamma rays, 1 with 4-MV photons, and 5 with 6-MV photons for the tangential fields. One breast was irradiated with an en-face electron beam. Seven patients with simultaneous breast cancer were treated by matched midline technique with bilateral tangential fields using the CT simulator (Fig 2). On the other hand, we referred to the CT simulation images of the first tumors to avoid field overlapping when we determined the tangential fields for the second tumors in the patients with metachronous breast cancers (Fig 3). The primary site was boosted in the 7 patients with close or positive surgical margins. This boost irradiation comprised to a total dose of 10 Gy in 5 fractions of electron beams through a field 6 to 8 cm in diameter, including the tumor bed. The ipsilateral supraclavicular and ipsilateral internal mammary nodal areas were not included in the target volume.

All patients received oral 5-fluorouracil (5-FU) or its derivatives, and also received tamoxifen for 2 years after the operation, regardless of the axillary node status or estrogen receptor (ER) status.

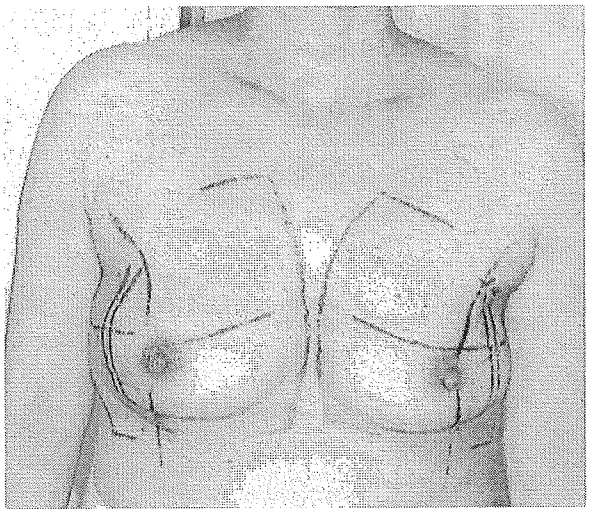

Fig 2. A case of simultaneous breast cancer: It is confirmed that there is no overlap by the skin markings.

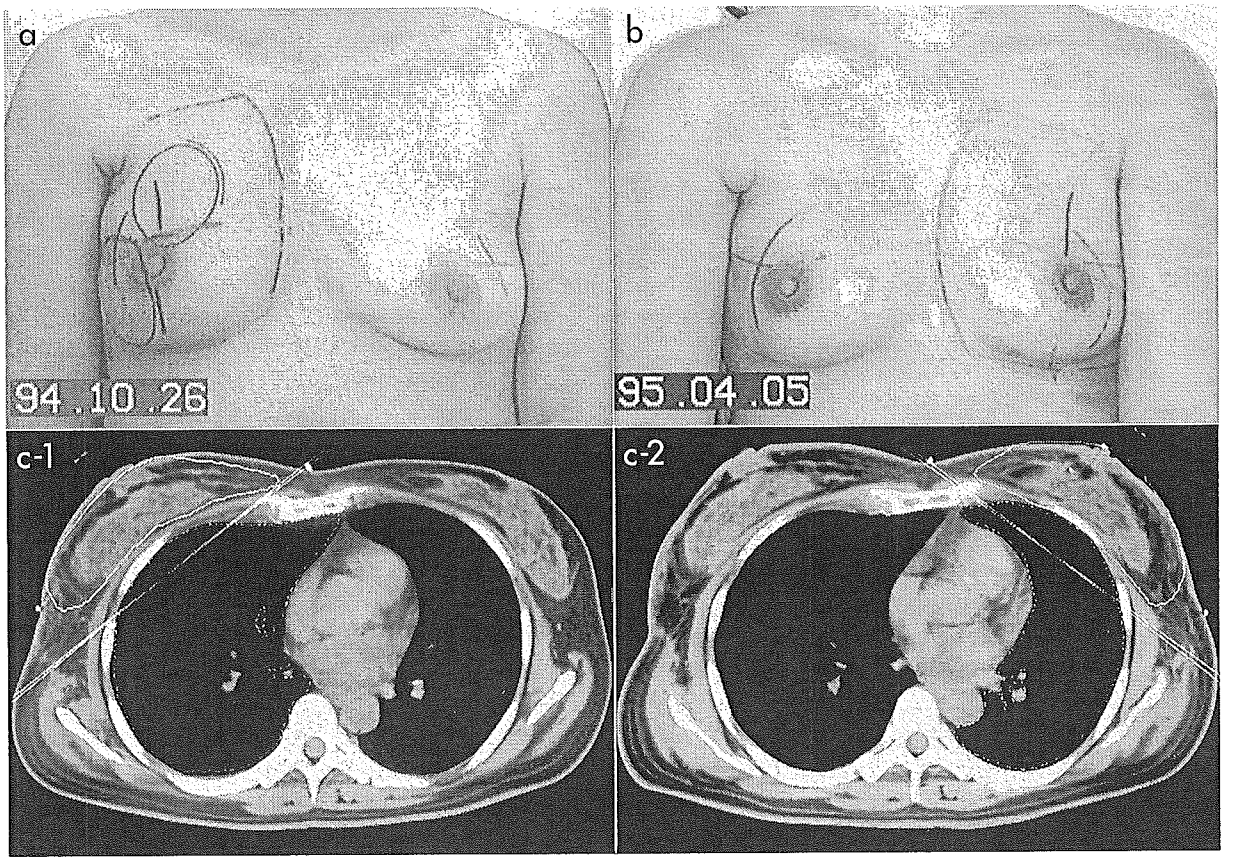

Fig 3. A case of metachronous breast cancer. (a) Radiation field for the first treatment. (b) Radiation field for the second treatment. Identifying the first field by the skin reaction is impossible. (c) We could recognize the first field accurately with the use of images from the previous CT simulation.

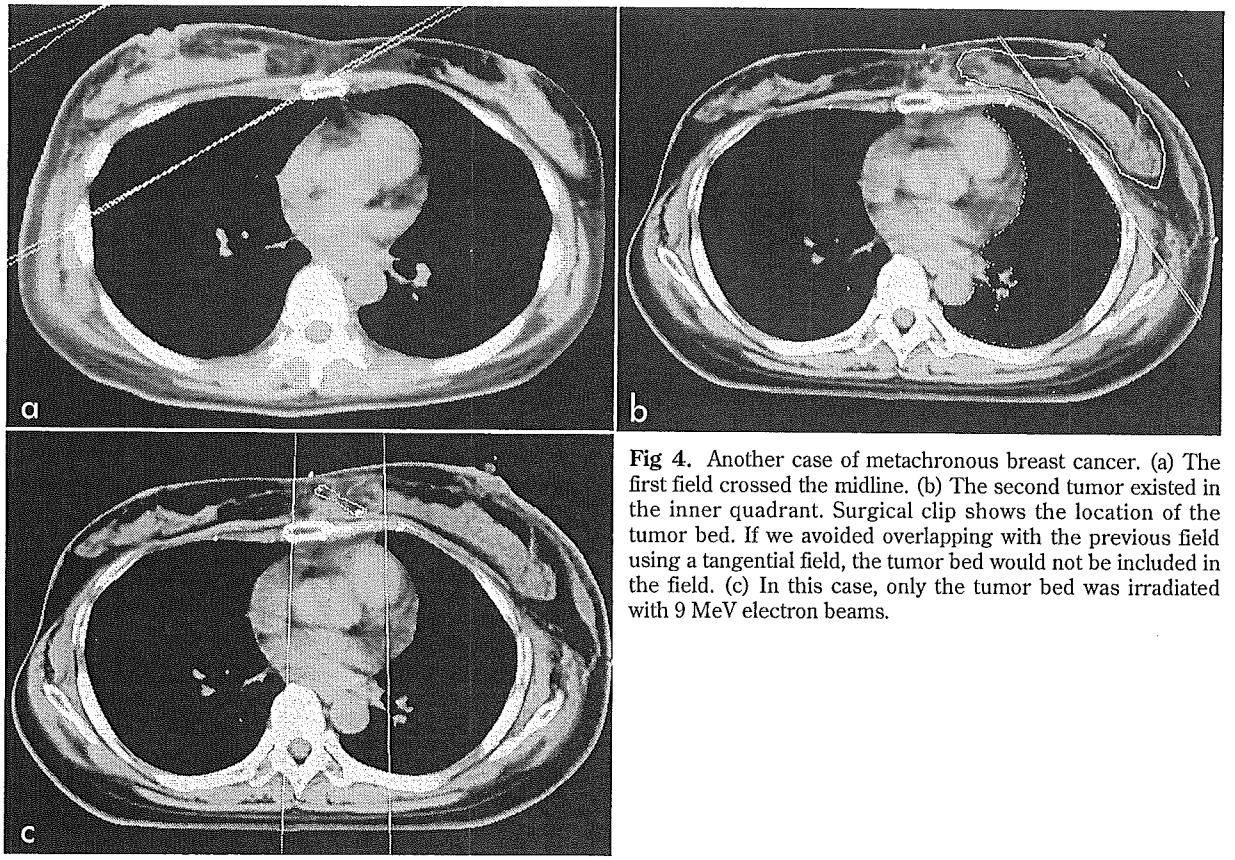

Fig 4. Another case of metachronous breast cancer. (a) The first field crossed the midline. (b) The second tumor existed in the inner quadrant. Surgical clip shows the location of the tumor bed. If we avoided overlapping with the previous field using a tangential field, the tumor bed would not be included in the field. (c) In this case, only the tumor bed was irradiated with 9 MeV electron beams.

The patients were periodically followed-up at our clinic. They were examined every 3 to 6 months in the first 2 years, and every 6 to 12 months thereafter according their pathological status. Loco-regional recurrence, distant metastasis, complications and cosmetic outcomes were evaluated.

Results

Of 17 patients, 15 patients were irradiated with matched tangential fields without overlapping, 1 patient was irradiated iwith matched tangential fields with overlapping of 1.2 cm, and 1 patient with a medially located metachronous tumor received en-face electron beam alone because overlapping with the previous field could not be avoided with tangential field (Fig 4).

No patients were lost to follow-up. The median follow-up period after each operation was 95 months. No patients showed loco-regional recurrence on either side or distant metastasis.

Regarding complications associated with treatment, severe arm edema was observed in one patient whose upper arms showed a 4 cm difference in circumference. One patient developed moderate fibrosis at the site of overlapping, but this did not affect cosmetic outcome. The patient who was irradiated with overlapping of 1.2 cm did not develop any skin or soft tissue complications. In other cases, complications were none or slight.

We also evaluated cosmetic outcome using the cosmetic score[7]. Six patients (35%) were scored as excellent and 10 (59%) were scored as good. Only one patient (6%) was graded fair because of unilateral breast contracture.

Discussion

Although as many as 10% of the patients with breast cancer may develop bilateral cancer[1-3] and radiation therapy is essential to breast conserving therapy, there is scant information on the technical aspects of such irradiation[8,9]. To minimize late damage to skin and soft tissue, overlapping of bilateral tangential fields should be avoided. On the other hand, maintaining good coverage of breast tissue is important to minimize the risk of intra-breast recurrence. In the patients with meta-

chronous breast cancer patients, which account for 2/3 of all bilateral cases, it is necessary to reproduce the previous tangential field before planning the contralateral tangential beam. In a conventional X-ray simulator, it is almost impossible to reproduce the medial margin accurately. Tattooing, which is commonly used in Western countries and might be useful in such situations, is seldom used in Japan. CT-simulation is quite useful because the overlapping of bilateral tangential fields can be evaluated much more accurately than conventional simulation, although there are some limitations derived from the change of the patient's figure and the difference in positioning. In patients with thick subcutaneous tissue at the midline, or those with tumors located very near to the midline, overlapping may be unavoidable despite the use of a CT simulator. However, it is still possible to explore the use of a CT for planning tangential fields for irradiation of metachronous breast cancer patients.

Conclusion

This study demonstrated that BCT is feasible for bilateral breast cancer and the CT simulator is useful for determining the radiation field, especially when they are metachronous. It is helpful in minimizing overlap of the radiation fields and provides the best possible treatment plan.

References

1) Donovan AJ: Bilateral breast cancer. *Surg Clin North Am* 70:1141-1149, 1990.
2) Gogas J, Markopoulos C, Skandalakis P, *et al*: Bilateral breast cancer. *Am Surg* 59:733-735, 1993.
3) Michowitz M, Noy S, Lazebnik N, *et al*: Bilateral breast cancer. *J Surg Oncol* 30:109-112, 1985.
4) van Limbergen E, van den Bogaert W, van der Schueren E, *et al*: Tumor excision and radiotherapy as primary treatment of breast cancer. Analysis of patient and treatment parameters and local control. *Radiother Oncol* 8:1-9, 1987.
5) Chu AM, Cope O, Russo R, *et al*: Patterns of local-regional recurrence and results in Stages I and II breast cancer treated by irradiation following limited surgery. An update. *Am J Clin Oncol* 7:221-229, 1984.
6) Bedwinek JM, Brady L, Perez CA, *et al*: Irradiation as the primary management of stage I and II adenocarcinoma of the breast: analysis of the RTOG breast registry. *Cancer Clin Trials* 3:11-18, 1980.
7) Harris JR, Levene MB, Svensson G, *et al*: Analysis of cosmetic results following primary radiation therapy for stages I and II carcinoma of the breast. *Int J Radiat Oncol Biol Phys* 5:257-261, 1979.
8) Kopelson G, Munzenrider JE, Doppke K, *et al*: Bilateral breast cancer: radiation therapy results and technical considerations. *Int J Radiat Oncol Biol Phys* 7:335-341, 1981.
9) Fung MC, Schultz DJ, Solin LJ: Early-stage bilateral breast cancer treated with breast-conserving surgery and definitive irradiation: the University of Pennsylvania experience. *Int J Radiat Oncol Biol Phys* 38:959-967, 1997.

Int J Clin Oncol (2005) 10:398–404
DOI 10.1007/s10147-005-0519-4

ORIGINAL ARTICLE

SuYu Zhu · Takashi Mizowaki · Yasushi Nagata
Kenji Takayama · Yoshiki Norihisa · Shinsuke Yano
Masahiro Hiraoka

Comparison of three radiotherapy treatment planning protocols of definitive external-beam radiation for localized prostate cancer

Received: March 17, 2005 / Accepted: July 7, 2005

Abstract
Background. Three radiotherapy treatment planning (RTTP) protocols for definitive external-beam radiation for localized prostate cancer, designed and clinically applied at Kyoto University, were compared.
Methods. Treatment plans were created according to three different RTTP protocols (old three-dimensional conformal radiotherapy [3D-CRT], new 3D-CRT, and intensity-modulated radiotherapy [IMRT]) on computed tomography (CT) data sets of five patients with localized prostate cancer. The dynamic-arc conformal technique was used in the 3D-CRT protocols. Differences in dose distribution were evaluated and compared based on dose-volume histogram (DVH) analyses.
Results. The coverage of the clinical target volume (= prostate alone) was comparable among the three RTTP protocols. However, the average values for the percent volume that received at least 95% of the prescription dose (V95), the percent of the prescription dose covering 95% of the volume (D95), and the conformity index of the planning target volume (PTV) were 99%, 97%, and 0.88 for the IMRT; 93.9%, 94.5%, and 0.76 for the new 3D-CRT; and 59.6%, 82.9%, and 0.6 for the old 3D-CRT protocol, respectively. Inhomogeneity of doses to the PTV was larger with the IMRT protocol than with the new 3D-CRT protocol. Doses to both the rectal wall and bladder wall were almost comparable with the new 3D-CRT and IMRT protocols, but were lower with the old 3D-CRT protocol, due to the lowest prescription dose and incomplete dose coverage of the PTV.
Conclusion. The old 3D-CRT protocol could not achieve the goals for the PTV set in the IMRT protocol. The new 3D-CRT and IMRT protocols were generally comparable in terms of both the PTV coverage and normal tissue-sparing, although the IMRT protocol achieved the most conformal dose distribution to the PTV, in return for a larger, but acceptable, dose inhomogeneity.

Key words Intensity-modulated radiotherapy · Dynamic-arc conformal radiotherapy · Prostate cancer · Radiotherapy treatment planning

S.-Y. Zhu · T. Mizowaki (✉) · Y. Nagata · K. Takayama · Y. Norihisa · S. Yano · M. Hiraoka
Department of Radiation Oncology and Image-Applied Therapy, Graduate School of Medicine, Kyoto University, 54 Shogoin-Kawahara-cho, Sakyo-ku, Kyoto 606-8507, Japan
Tel. +81-75-751-3762; Fax +81-75-771-9749
e-mail: mizo@kuhp.kyoto-u.ac.jp

Introduction

Although external-beam radiotherapy with definitive intent is widely applied in patients with localized prostate cancer in Western countries, surgical treatment had been the mainstream in Japan for a long time. However, this situation has gradually changed as the outcomes of radiotherapy were reported to be comparable to those of surgery.[1,2] At Kyoto University, three-dimensional conformal radiotherapy (3D-CRT) was initiated in 1997 as definitive treatment for localized prostate cancer (T1-2N0M0), with a prescription dose of 70 Gy (old 3D-CRT protocol). However, this radiotherapy treatment planning (RTTP) protocol was designed by adding relatively small multileaf collimator (MLC) margins directly to the clinical target volume (CTV), because the first priority was given to reducing the rectal toxicity, in order to recruit patients from the surgical side. As a matter of fact, if the planning target volume (PTV) were to have been created according to the definition set in the current RTTP protocols (new 3D-CRT and intensity-modulated radiotherapy [IMRT] protocols), the dose coverage of the PTV in the old 3D-CRT protocol would be regarded as insufficient.

Recently, several dose escalation studies have suggested that escalating the dose to 72–78 Gy would be beneficial for patients with localized prostate cancer, in terms of prostate-specific antigen (PSA) failure-free survival rate.[3–7] In addition, an even higher dose can be delivered safely with the latest sophisticated radiotherapy technique, IMRT, in which a higher local control rate was achieved by higher

Table 1. Patients' characteristics

Stage (UICC 2002)	
T1c	n = 3
T2b	n = 1
T2c	n = 1
Prostate (CTV) volume, in ml	Median, 29.2 (24–62.5)
Rectal wall volume, in ml	Median, 41.9 (35.9–55.7)
PTV volume, in ml	Median, 91.5 (73.3–155.5)

Figures in parentheses in Tables 1 and 3 are ranges

dose delivery, based on pathological evaluations of biopsy specimens after radiation to the prostate.[8–11]

In November 2000, we started applying IMRT in patients with localized prostate cancer as a pilot study, followed by a phase I dose escalation study. By December 2002, we had established RTTP protocols using IMRT (IMRT protocol) and a dynamic-arc conformal 3D-CRT technique (new 3D-CRT) with a prescription dose of 74 Gy.

In the present study, details of the three RTTP protocols are described, and differences in the target coverage and doses to the normal tissues among the three RTTP protocols are compared by analyzing the dose distributions and dose-volume histograms (DVH).

Patients and methods

Patients' characteristics

The Planning computed tomography (CT) data sets of five patients randomly chosen from the clinical data pool of patients with localized prostate cancer treated by external-beam radiotherapy at our institution were used in the present study. The patients' characteristics are indicated in Table 1.

Planning CT scans and contouring of structures

All planning CT scans were obtained by using a CT simulator (CTS-20; Shimadzu, Kyoto, Japan) with 5-mm slice thickness, without a gap from the iliac crest to 8 cm below the ischial tuberosities. Patients were instructed to void the bladder and rectum about 1–1.5 h before the CT simulation, according to their individual urinary conditions. Target delineations and treatment planning were performed with the Eclipse-Helios system (Ver. 7.1.35; Varian Medical System, Palo Alto, CA, USA).

The prostate, outer rectal wall, outer bladder wall, bilateral femurs, small bowel, and large bowel were contoured. The CTV was defined as the prostate alone and contoured in reference to the findings on magnetic resonance imaging (MRI) and/or retrograde urethrography. The PTV was created by adding the following margins in a 3D setting: a 9-mm margin universally, except for a 6-mm margin posteriorly and a 10-mm margin superiorly (in the cranial direction). The rectal wall was generated from the outer rectal wall, using a wall-extraction function with a wall thickness of 4 mm on every CT slice from 10 mm below the apex of the prostate to 10 mm above the tips of the seminal vesicles. The bladder wall was generated from the outer bladder wall in the same manner as the rectal wall, with a wall thickness of 4 mm. All plans were designed according to each planning protocol with 15-MV photon beams of Clinac 2100C or 2300 C/D (Varian Medical System). The final dose distributions for all plans were calculated using a pencil-beam convolution algorithm with a calculation grid resolution of 2.5 mm by 2.5 mm, in which the Modified Batho heterogeneity correction was applied.

Descriptions of the three RTTP protocols

Old 3D-CRT protocol

For the old 3D-CRT protocol, 46 Gy in 23 fractions was given by the four-field box technique, with MLC conformation to the CTV, followed by an additional 24 Gy in 12 fractions, with the dynamic-arc conformal technique. A PTV was not created in this RTTP protocol. In the four-field irradiation, the MLC edges were placed directly to the CTV with the margins of 12 mm in the superior/inferior directions and 7 mm in the remaining directions, based on the beam's eye-view of each field. If part of the posterior rectal wall was included in the lateral opposing fields, the MLC positions were manually adjusted to completely shield the posterior wall from the area irradiated by the bilateral fields. In dynamic-arc conformal radiotherapy, two lateral arcs of 100° of rotation (from 36° to 136°, and 226° to 326°) were used with dynamic conformal fitting of MLCs to the CTV with a 7-mm margin. This technique enables continuous beam delivery with dynamic changing of the MLC positions conforming to the target as the gantry rotates.[12] The prescription dose in the old 3D-CRT protocol was 70 Gy in 35 fractions at the center of the CTV, which was the isocenter of the fields. Patients were placed in the supine position without any fixation devices.

New 3D-CRT protocol

For the new 3D-CRT protocol, two lateral dynamic arcs with 100° of rotation (from 36° to 136° and 226° to 326°) were used by dynamic conformal fitting of MLCs to the PTV, in which a 3-mm margin was generally placed from the edge of the PTV to the tips of the MLCs. Seventy-four Gy was prescribed to the center of the CTV (= isocenter of the fields). Patients were placed in the supine position without any immobilization devices.

IMRT protocol

For the IMRT protocol, a five-field dynamic multileaf collimator (DMLC) technique was used. The beam arrangement was as follows: a posterior (0°), right posterior oblique (75°), right anterior oblique (135°), left anterior oblique (225°), and left posterior oblique field (285°). Inverse treatment planning by computer optimization[13,14] was used with

the Helios system (Varian Medical System). Inverse optimizations were performed until the following planning goals were completely satisfied. As for the PTV, D95 (see definition under "methods for plan comparison and evaluation") should generally be 95% (at least 90%) of the prescription dose, maximum dose should be 110% or less, V90 (see definition under heading cited above) should be 98% or higher, and the mean dose will generally be 102% of the prescription dose. For the rectal wall, no more than 1% of the rectal wall volume should receive more than the prescription dose, no more than 25% of the rectal wall volume should receive more than 70 Gy, no more than 35% of the rectal wall volume should receive more than 60 Gy, and no more than 60% of the rectal wall volume should receive more than 40 Gy. With respect to the bladder wall, no more than 60% of the bladder wall volume should receive more than 40 Gy and no more than 35% of the bladder wall volume should receive more than 70 Gy. With regard to the femoral head, the maximum dose to any point should be less than 60 Gy. For the small and large bowel, no more than 0.5 cc of the volume should receive more than 60 Gy and more than 65 Gy, respectively. In addition to the hard constraints described above, the following soft constraints were applied to the final dose distribution. (a) The anterior rectal wall should receive 90%–100% of the dose (the 95% isodose-line usually lies very close to the anterior border of the rectal wall). (b) No significant hot spots exist outside the PTV. (c) The 50% isodose-line of the prescription dose should generally not exceed the posterior wall of the rectum posteriorly. Patients were immobilized in the prone position using thermoplastic shells (Hip Fix System; Med-Tec, Orange City, IA, USA) covering from the mid-thigh to the upper-third of the leg, with the combination of a vacuum pillow (Vac-Lok system; Med-Tec) and a leg support.

Methods for plan comparison and evaluation

The old 3D-CRT, new 3D-CRT, and IMRT plans were created according to each RTTP protocol for the five planning CT data sets. All plans were experimentally created on CT data sets used for the corresponding IMRT plan scanned with the patient in the prone position, so that the comparison among the three plans could be done based on the same CT data set. Therefore, the beam arrangements in the old 3D-CRT and the new 3D-CRT protocols were reversed in the ventral-dorsal direction in order to duplicate the planned dose distribution for the supine position on the CT data scanned in the prone position. Doses to the targets (CTV and PTV) and organs at risk (rectal and bladder wall) were evaluated and compared among the three different RTTP protocols, based on DVH analyses. V95 was defined as the percent volume that received at least 95% of the prescription dose. D95 was defined as the percent of the prescription dose covering 95% of the volume. Inhomogeneity in doses of the PTV was defined as $(D_5 - D_{95})/D_{mean}$.[15] The dose conformity to the PTV was calculated using the conformity index (CI) equation advocated by Van'Riet et al.[16] Here, the CI is defined as the product of the fraction of the PTV receiving at least 95% of the prescription dose and the ratio of the volume of the PTV receiving at least 95% of the prescription dose to the volume receiving at least 95% of the prescription dose, as shown in the equation: conformity index = $V_{PTV95\%}/V_{PTV} * V_{PTV95\%}/V_t$. Here, $V_{PTV95\%}$ is the PTV volume covered by 95% of the prescription dose, V_{PTV} is the volume of the PTV, and V_t is the body volume covered by 95% of the prescription dose. Therefore, the CI accounts for both any normal tissue volume receiving at least 95% of the prescription dose and for any volume of the PTV receiving less than 95% of the prescription dose.

Results

Coverage of the target volumes

Figure 1a indicates the mean DVHs of the CTV for the three different RTTP protocols. The CTV doses are summarized in Table 2. The CTVs were completely covered by 95% of the prescription dose in all protocols. In addition, the D95 values were 100%, 98.4%, and 97.6% for the

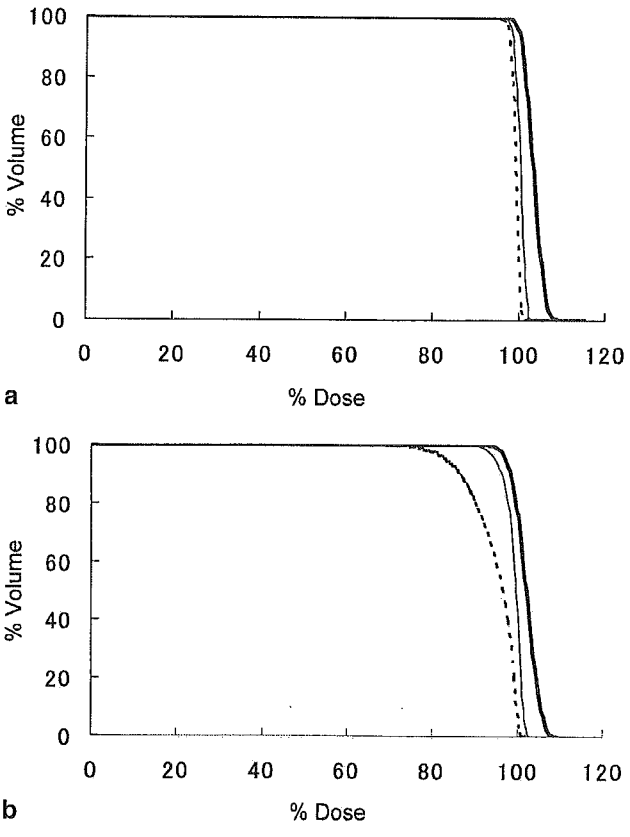

Fig. 1a,b. Mean dose-volume histograms (DVHs) of five patients for the clinical target volume (CTV; **a**) and planning target volume (PTV; **b**) by radiotherapy treatment planning (RTTP) protocols. The prescription dose was 70 Gy for the old three dimensional conformal radiotherapy (3D-CRT; *dashed line*) and 74 Gy for the new 3D-CRT (*thin continuous line*) and intensity-modulated radiotherapy (IMRT; *thick continuous line*) protocols

Table 2. RTPP results for the CTV

	IMRT (mean ± SD)	New 3D-CRT (mean ± SD)	Old 3D-CRT (mean ± SD)
V95 (%)	100 ± 0	100 ± 0	99.9 ± 0.1
D95 (%)	100 ± 0.9	98.4 ± 0.7	97.6 ± 0.6
Minimum dose (%)	98.1 ± 1.2	97 ± 0.6	95.3 ± 1.1
Maximum dose (%)	108.3 ± 1.8	102.6 ± 0.4	101.2 ± 0.5
Mean dose (%)	103.7 ± 0.7	100.7 ± 0.7	99.6 ± 0.3

V95, The percent volume receiving at least 95% of the prescription dose; D95, the least percent of the prescription dose covering 95% of the target volume; old 3D-CRT: 46-Gy box-fields + 24 Gy dynamic-arc conformal radiotherapy; new 3D-CRT, 74-Gy dynamic-arc conformal radiotherapy; IMRT, intensity-modulation radiotherapy

Table 3. RTPP results for the PTV

	IMRT (mean ± SD)	New 3D-CRT (mean ± SD)	Old 3D-CRT (mean ± SD)
V95 (%)	99 ± 0.5	93.9 ± 0.9	59.6 ± 6.8
D95 (%)	97 ± 0.5	94.5 ± 0.3	82.9 ± 1.5
Minimum dose (%)	87.7 ± 4.8	87.5 ± 0.7	60 ± 3.3
Maximum dose (%)	108.5 ± 1.8	102.6 ± 0.4	101.3 ± 0.5
Dose inhomogeneity (%)	8.8 ± 1	7.2 ± 0.7	18.2 ± 1.6
Mean dose (%)	102.3 ± 0.7	99.5 ± 0.3	94.9 ± 1
Conformity index	0.88 (0.87–0.89)	0.76 (0.72–0.78)	0.60 (0.52–0.65)

Conformity index = $V_{PTV95\%}/V_{PTV} * V_{PTV95\%}/Vt$; dose inhomogeneity = (D5 – D95)/Mean dose * 100; V95, the volume receiving at least 95% of the prescription dose; D95, the least percentage of the prescription dose covering 95% of the target volume; old 3D CRT, 46 Gy box-fields + 24 Gy dynamic arc conformal radiotherapy; new 3D CRT, 74 Gy dynamic-arc conformal radiotherapy; IMRT, intensity modulation radiotherapy

IMRT, new 3D-CRT, and old 3D-CRT protocols, respectively. Therefore, the coverage for the CTV of the three protocols was considered to be almost comparable, although the mean dose of the CTV was higher in IMRT cases compared with that in the 3D-CRT cases. Figure 1b shows the mean DVHs of the PTV for the three protocols. The PTV coverage was apparently worse with the old 3D-CRT protocol compared with the other two protocols, in which less than 60% of the PTV had received more than 95% of the prescription dose; only 83% of the prescription dose was delivered to 95% of the PTV; the dose inhomogeneity was more than double that in the other two protocols, and the conformity index was the worst (0.6 on average). The DVH statistics of the PTV are summarized in Table 3. Both V95 and D95 for IMRT and the new 3D-CRT plans were considered to be acceptable, because 95% of the PTV was covered by 95% of the prescription dose, although both indexes were slightly better in the IMRT protocol. The dose inhomogeneity of the PTV in the IMRT protocol was larger than that for the new 3D-CRT plan (Table 3). On the other hand, the conformity index of the IMRT plan was the highest (0.88 on average) among the three RTTP protocols, indicating that the dose distribution for the IMRT protocol was most conformal to the target among the three RTTP protocols evaluated in the present study.

Doses to organs at risk

Figure 2a,b shows the mean DVHs of the five cases for the rectal wall (Fig. 2a) and bladder wall (Fig. 2b). The percent volumes of the rectal and bladder walls receiving 25, 40, 60, and 70 Gy or higher with each protocol are listed in Tables 4 and 5, respectively. Both the rectal and bladder wall doses in the cases with the old 3D-CRT were lowest, due to the lowest total prescription dose and insufficient dose coverage of the PTV. The percent rectal wall volume irradiated to 25 Gy for the IMRT cases was higher than that for the cases with the new 3D-CRT. The differences in the percent rectal wall volumes irradiated to 40, 60, and 70 Gy between the cases with IMRT and the cases with new 3D-CRT were very small (1%–3% differences). Table 5 demonstrates that

Table 4. Comparison of the percent rectal wall volumes at each dose level for the IMRT, new 3D-CRT, and old 3D-CRT protocols

Dose (Gy)	IMRT (mean ± SD)	New 3D-CRT (mean ± SD)	Old 3D-CRT (mean ± SD)
25	83.1 ± 11.7	61.8 ± 9.3	50.2 ± 23.2
40	46.9 ± 10.7	42.5 ± 5.7	31.9 ± 15.5
60	20.9 ± 6.1	23.3 ± 3.0	17.5 ± 9.0
70	9.1 ± 4.0	10.6 ± 1.5	0

Table 5. Comparison of the percent bladder wall volumes at each dose level for the IMRT, new 3D-CRT, and old 3D-CRT protocols

Dose (Gy)	IMRT (mean ± SD)	New 3D-CRT (mean ± SD)	Old 3D-CRT (mean ± SD)
25	54.3 ± 15.6	65.4 ± 18.9	50.2 ± 23.2
40	39.2 ± 11.6	51.4 ± 18.1	31.9 ± 15.5
60	24.8 ± 7.6	34.6 ± 15.4	17.5 ± 9.0
70	16.8 ± 5.0	22.8 ± 10.9	0

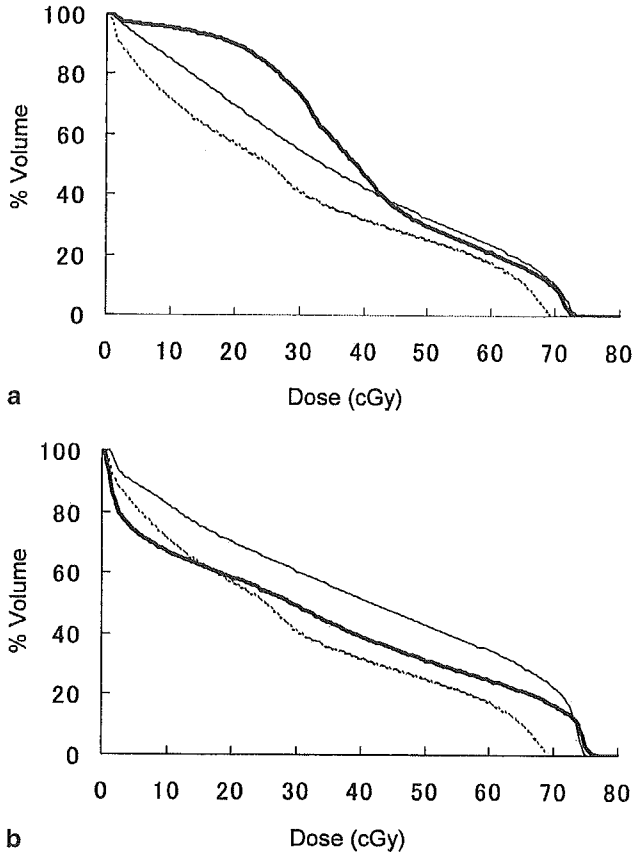

Fig. 2a,b. Mean DVHs of five patients for the rectal wall (**a**) and bladder wall (**b**) by RTTP protocols. The prescription dose was 70 Gy for the old 3D-CRT (*dashed line*), and 74 Gy for the new 3D-CRT (*thin continuous line*), and IMRT (*thick continuous line*) protocols

the doses to the bladder wall in IMRT cases were lower than those in the new 3D-CRT cases.

Evaluation of the dose distribution

Figure 3 shows examples of the dose distribution in the three protocols. Even with the IMRT protocol, there was no significant hot spot outside the PTV, despite the well-balanced dose distribution between the PTV and the normal structures. In addition, the dose conformity was apparently better with the IMRT compared with the other protocols.

Discussion

The data of this study corroborate findings that the design of the old 3D-CRT protocol was not able to generate the qualified dose coverage to the PTV that is currently applied at our institute. The main reason for this is that the protocol was originally designed to set relatively smaller MLC margins directly to the CTV without creating the PTV, because the old 3D-CRT protocol was designed during the period of

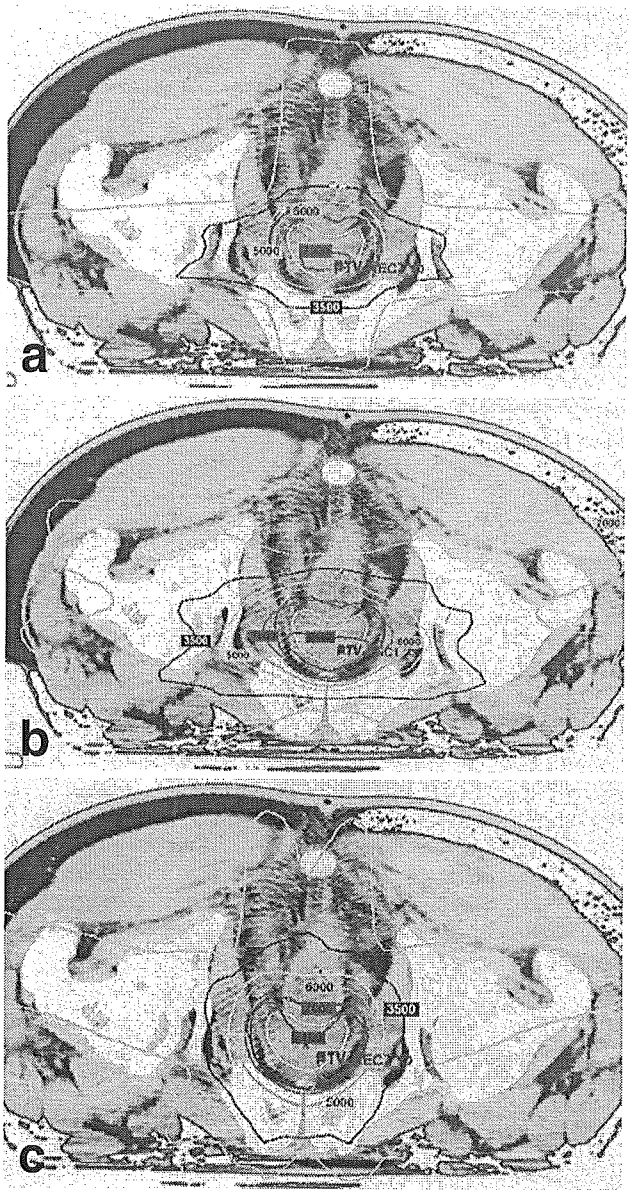

Fig. 3a–c. Examples of dose distribution with the old 3D-CRT (**a**), new 3D-CRT (**b**), and IMRT protocols (**c**)

transition from two-dimensional treatment planning to 3D-CRT, and aimed to give first priority to reducing normal-tissue doses in order to recruit patients from the surgery side.

On the other hand, the new 3D-CRT protocol achieved the RTTP goals set in the IMRT protocol, including coverage of the PTV. The dynamic-arc conformal radiotherapy technique has been developed in Japan, and is widely used all over the country. It automatically changes the MLC shape to conform to the target as the gantry rotates. Through trial and error, we found that the two arcs of 36°–136° and 226°–326° were the most appropriate beam arrangements for localized prostate irradiation, as a class solution. Therefore, the planning process is not as heavily

dependent on the planner's expertise as is the other 3D-CRT technique. Because the new 3D-CRT technique can realize better PTV dose coverage than the old 3D-CRT does (Fig. 1b; Table 3), it is hoped that a higher biochemical control rate at 3 and 5 years can be achieved for this group of patients to be treated by the new 3D-CRT technique. Our data showed that the PTV coverage of the new 3D-CRT was slightly inferior to that of the IMRT protocol. However, the planning and delivery time with the IMRT protocol is longer than that with the new 3D-CRT protocol. The approximate times required for treatment planning, including contouring, optimization, and dose calculation for the old 3D-CRT, new-3D-CRT, and IMRT were 1.5–2 h, 1.0–1.5 h, and 1.5–2 h, respectively. The approximate times for each delivery, including patient setup, gantry rotation, and beam-on time, were 6–10 min, 5–7 min, and 10–15 min for the old 3D-CRT, new-3D-CRT, and IMRT protocols, respectively. In addition, as the process of quality assurance for the IMRT protocol is very labor-intensive at this point, the available IMRT resources at our institution are currently very limited. Therefore, we decided to mainly apply IMRT to intermediate- or high-risk groups of patients who were expected to receive a greater benefit from higher-dose irradiation to both the prostate and the seminal vesicles, for which IMRT is expected to demonstrate its true abilities.

Our current PTV definition was created based on experiences at other institutions reported in the literature,[3,5,11,17,18] in combination with our experiences with the old 3D-CRT protocol. In fact, the margins added to the CTV to create the PTV (PTV margins) were almost the same as those applied at the Memorial Sloan-Kettering Cancer Center (MSKCC). Although a report from the MSKCC has indicated that the current PTV margins are not enough to include the CTV all the time,[19] high-dose irradiation with the present PTV margins can be justified by the very promising clinical outcomes achieved at the MSKCC.[8,11]

There is a trade-off in the IMRT protocal between the target dose inhomogeneity and the sparing of organs at risk.[10] In fact, the IMRT protocol achieved slightly better dose coverage of the PTV, but resulted in higher dose inhomogeneity within the PTV, than the new 3D-CRT protocol, as indicated in the present study (Fig. 1; Tables 2–5). Conceptually, IMRT can generate dose distribution for the PTV that is at least comparable, in terms of both dose homogeneity and coverage, to that generated by the conventional 3D-CRT protocol, as long as other constraints to organs at risk are the same. However, in most of the patients in whom our IMRT protocol was used, the first priority was usually given to the sparing of organs at risk over achieving better homogeneity in the target dose, which resulted in a higher dose heterogeneity in the PTV for the IMRT protocol than for the 3D-CRT protocol. However, the maximum limit of 110% of the prescription dose in our IMRT protocol is a widely accepted limit for both the 3D-CRT and IMRT protocols.

As for the methods of evaluation of the planning results, DVH analyses alone is not enough, because DVH itself cannot account for the doses to the nondelineated tissues, which may result in undetected hot spots outside the contoured regions. In addition, DHV cannot indicate the location of hot spots or cold spots within the delineated volumes. If a hot spot is deposited in the tumor-bearing region, it may contribute to improving the tumor control. On the other hand, when hot spots happen to reside in the urethra, they may cause urinary toxicity. The consequences of this issue are still controversial and are not fully understood in the actual clinical situation.[10] In addition, continued technological advances in biological-based image-guided therapy may provide the capacity to point the dose to the tumor-bearing region without creating hot spots in normal structures.

Our results demonstrated that our dynamic-arc conformal approach is not apparently inferior to the IMRT protocol, in terms of rectal sparing when irradiating the prostate alone. However, our pilot evaluation suggested that, for the treatment of both the prostate and seminal vesicles, IMRT can provide a much better solution, in terms of target coverage and rectal sparing, than dynamic conformal-arc 3D-CRT (data not shown). In fact, Zelefsky et al.[11] compared a 3D-CRT protocol of six co-planar fields with a five-field dynamic multileaf collimator IMRT protocol for delivering 81 Gy to both the prostate and entire seminal vesicles, and demonstrated that IMRT could significantly reduce the percent volume of the rectal wall at doses between 50 and 77 Gy.

In conclusion, dynamic-arc 3D-CRT (new 3D-CRT protocol) is generally comparable to the IMRT protocol in terms of both target coverage and rectal sparing when irradiating the prostate alone. Therefore, dynamic-arc conformal radiotherapy can be a good alternative to IMRT, although long-term results for tumor control and complication rates still need to be verified to confirm whether the results of this planning study can be extrapolated to clinical outcomes. Our IMRT and dynamic-arc 3D-CRT approaches are much superior to the old 3D-CRT protocol in terms of the PTV coverage, and these newer approaches are expected to lead to better probability of tumor control.

Acknowledgments This work was supported in part by Sasagawa Japan–China Medical Association Scholarship, Sagawa Foundation for Promotion of Cancer Research, and a Grant-In-Aid for Scientific Research from The Ministry of Education, Culture, Sport, Science, and Technology of Japan (Exploratory Research: no. 16659316).

References

1. Fowler JE Jr, Braswell NT, Pandey P, et al. (1995) Experience with radical prostatectomy and radiation therapy for localized prostate cancer at a Veterans Affairs Medical Center. J Urol 153: 1026–1031
2. Keyser D, Kupelian PA, Zippe CD, et al. (1997) Stage T1–2 prostate cancer with pretreatment prostate-specific antigen level ≤10 ng/ml: radiation therapy or surgery? Int J Radiat Oncol Biol Phys 38:723–729
3. Leibel SA, Heimann R, Kutcher GJ, et al. (1993) Three-dimensional conformal radiation therapy in locally advanced carcinoma of the prostate: preliminary results of a phase I dose-escalation study. Int J Radiat Oncol Biol Phys 28:55–65

4. Hanks GE, Schultheiss TE, Hanlon AL, et al. (1997) Optimization of conformal radiation treatment of prostate cancer: report of a dose escalation study. Int J Radiat Oncol Biol Phys 37:543–550
5. Zelefsky MJ, Leibel SA, Gaudin PB, et al. (1998) Dose escalation with three-dimensional conformal radiation therapy affects the outcome in prostate cancer. Int J Radiat Oncol Biol Phys 41:491–500
6. Michalski JM, Purdy JA, Winter K, et al. (2000) Preliminary report of toxicity following 3D radiation therapy for prostate cancer on 3DOG/RTOG 9406. Int J Radiat Oncol Biol Phys 46:391–402
7. Pollack A, Zagars GK (1997) External beam radiotherapy dose response of prostate cancer. Int J Radiat Oncol Biol Phys 39:1011–1018
8. Zelefsky MJ, Fuks Z, Hunt M, et al. (2002) High-dose intensity modulated radiation therapy for prostate cancer: early toxicity and biochemical outcome in 772 patients. Int J Radiat Oncol Biol Phys 53:1111–1116
9. Burman CM, Chui CS, Kutcher GJ, et al. (1997) Planning, delivery, and quality assurance of intensity-modulated radiotherapy using dynamic multileaf collimator: a strategy for large-scale implementation for the treatment of carcinoma of the prostate. Int J Radiat Oncol Biol Phys 39:863–873
10. Intensity Modulated Radiation Therapy Collaborative Working Group (2001) Intensity-modulated radiotherapy: current status and issues of interest. Int J Radiat Oncol Biol Phys 51:880–914
11. Zelefsky MJ, Fuks Z, Happersett L, et al. (2000) Clinical experience with intensity modulated radiation therapy (IMRT) in prostate cancer. Radiother Oncol 55:241–249
12. Nagata Y, Okajima K, Murata R, et al. (1996) Development of an integrated radiotherapy network system. Int J Radiat Oncol Biol Phys 34:1105–1111
13. Bortfelt T, Kahler DL, Waldron TS, et al. (1994) X-ray field compensation with multileaf collimators. Int J Radiat Oncol Biol Phys 28:72–73
14. Mohan R, Wang X, Jackson A, et al. (1994) The potential and limitations of the inverse radiotherapy technique. Radiother Oncol 32:232–248
15. Mock U, Georg D, Bogner J, et al. (2004) Treatment planning comparison of conventional, 3D conformal, and intensity-modulated photon (IMRT) and proton therapy for paranasal sinus carcinoma. Int J Radiat Oncol Biol Phys 58:147–154
16. Van'Riet MS, Mak ACA, Moerland MA, et al. (1997) A conformation number to quantify the degree of conformality in brachytherapy and external beam irradiation: application to the prostate. Int J Radiat Oncol Biol Phys 37:731–736
17. Zelefsky MJ, Cowen D, Fuks Z, et al. (1999) Long term tolerance of high dose three dimensional conformal radiotherapy in patients with localized prostate cancer. Cancer 85:2460–2468
18. Boersma LJ, van den Brink M, Bruce AM, et al. (1998) Estimation of the incidence of late bladder and rectum complications after high-dose (70–78 Gy) conformal radiotherapy for prostate cancer using dose-volume histograms. Int J Radiat Oncol Biol Phys 41:83–92
19. Chiaho Hua D, Lovelock M, Mageras GS, et al. (2003) Development of a semi-automatic alignment tool for accelerated localization of the prostate. Int J Radiat Oncol Biol Phys 55:811–824